A Synchronization Protocol for Multi-User Cell Signaling-Based Molecular Communication

Ligia F. Borges,* **Michael T. Barros**,† **Michele Nogueira**‡
*NR2 - Federal University of Paraná, Brazil
† School of Computer Science and Electronic Engineering, University of Essex, UK
‡ Department of Computer Science, Federal University of Minas Gerais, Brazil
Emails: lfborges@inf.ufpr.br, m.barros@essex.ac.uk, michele@dcc.ufmg.br

***Abstract*—Molecular Communications (MC) networks comprise multiple devices performing coordinated complex tasks, such as detecting types of cancer and smart drug delivery. Signaling-based MC uses molecules as information carriers between signaling cells. In this context, synchronization is jointly paramount and challenging since the system must overcome the limitation of molecular propagation to make sure computationally deprived bio-devices can communicate. On top of that, a multi-user increases this system challenges as possible co-channel interference causes errors or failures. Bio-devices present severe computational and communication limitations, being this last one essentially unidirectional. This paper presents the first synchronization protocol between signaling cells for multi-user MC. Results have shown the convergence time concerning different network sizes from 12 to 60 nodes.**

***Index Terms*—synchronization, cellular-signaling channel, molecular communication**

I. Introduction

Intra-body networks leverage new applications in nanomedicine with remarkable results, including bio-devices to monitor glucose and cholesterol, infectious agent detection, or cancer identification [1]. The research community has adopted distinct elements of biochemical processes and has abstracted them into models to design systems following the molecular communication (MC) paradigm. The main example is the natural signaling process of human body cells, which can exchange information based on the transmission, propagation, and reception of molecules through biochemical and physical processes. This paper focuses on cell signaling-based MC govern by reaction-diffusion processes for cell-to-cell communication mediated by gap junctions.

The current literature on signaling-based cell-to-cell communication focuses mainly on single-user approaches. The works focused on modeling and analyze the communication channel and its particularities, such as molecules, gap junctions, chemical reactions, cellular tissues, noise, and other elements of natural communication [2]–[5]. Efficient communication is truly achieved when synchronization is achieved, and the main challenge is that MC relies on computationally deprived devices or biological circuits where clocks are not fine-tuned for communications as in digital systems. There are few works addressing time synchronization [6], [7], or other means of efficient communications, including symbol synchronization [8] and interference mitigation [9]. However, those works focus on a different type of MC that is not in the scope of this work, in which the molecules are suspended in a fluid and move randomly in the absence of chemical reactions. Also, those works assume a two-way communication between nanomachines, which is not the case for cell signaling-based channels, as they are essentially unidirectional.

Bio-devices operate in a shared small-scaled environment to perform complex tasks and collaborative work. Although single-user MC has been extensively studied for cellular tissues, designing multi-user MC systems is necessary to support the full operation of MC networks. However, they still depend on several advancements, including feasible synchronization schemes that fit the limitations of MC systems. Multi-user interferences, resulted from molecules emitted by other devices cause errors or failures in communication, being synchronization a crucial requirement to mitigate them.

This paper presents a synchronization protocol for multi-user cellular signaling-based networks. The protocol follows the premise that there is a bio-device playing the role of the main node. It releases beacons which are recognized as synchronization requests by bio-devices. Each transmitter records the reception time between signals and estimates the delay to adjust an internal timed process. The internal timer is bound to an oscillator that manages the release of molecules by type/concentration. The protocol considers the natural molecular diversity and their non-linear relationships as a leading alternative to reduce error and achieve low complexity.

Simulation scenarios consider a 3D astrocyte tissue, one of the most abundant cells in the central nervous system. Cellular reactions follow a stochastic algorithm [10] coupled with the intercellular reaction-diffusion process. This algorithm was used in our previous work [11] employed to simulate cellular tissue MC channels. Results show that the proposed protocol allows a network of sixty bio-devices to achieve convergence in terms of synchronization.

The paper proceeds as follows. Section II overviews the related works. Section III describes the proposed synchronization protocol. Section IV describes the evaluation method and discusses the results. Finally, Section V concludes the paper.

The authors thank CAPES, grant #88882.382196/2019-01, and CNPq, grants #313844/2020-8 and #426701/2018-6, for the support to this research.

II. Related Works

Synchronization techniques for MC follow in general resonance-based approach instead of the conventional clock synchronization one. In [9], the authors proposed a synchronization scheme by inhibitory molecules. A molecular machine propagates these molecules that inhibit the release of information molecules from other machines. When the concentration of information molecules falls below a certain threshold, it can be released. In [8], the authors proposed a symbol synchronization for free-diffusion systems that employ two types of molecules, one for synchronization and another for data transmission. Machines do not store the synchronization molecules but synthesize the corresponding type of molecule whenever a time interval is necessary for transmitting bits. The information molecules are detected during the interval when the number of synchronization molecules is above a threshold.

In [7], the authors presented a clock synchronization algorithm that uses a maximum likelihood estimate between two nanomachines. It considers the molecule synthesis time and occurs with a two-way message exchange mechanism between two nanomachines that exchange their propagation delay time. In [6], the authors proposed a time-slotted MC system with two synchronization schemes sender-initiated time-slot alignment and receiver-initiated time-slot alignment. The operation consists of a few signal exchanges between sender and receiver, without using timestamps. The technique estimates delay and the beginning of a time-slot at which the signal is expected to arrive.

The existing synchronization approaches bring initial ideas for the construction of multi-user MC networks. However, they are not suitable for cell signaling-based systems that have specific characteristics of propagation (*i.e.*, reaction-diffusion mediated by gap junctions), application (*e.g.*, identification and treatment of cellular tissue pathology), and cell-based network entities (*e.g.*, astrocytes, epithelial, and smooth muscle). For cellular signaling, the synchronization protocol must consider the unidirectional characteristic of the communication due to the stochastic diffusion direction of molecules in gap junction channels that restricts techniques based on the exchange of bidirectional messages and the computational restrictions of the bio-devices.

III. Synchronization Protocol for Multi-User Molecular Communications

This section details the proposed synchronization protocol for multi-user cell signaling-based networks. The protocol design assumes a network model in which two or more bio-devices communicate through MC within tissues (Fig. 1). The intracellular MC relies on signaling pathways, i.e., a network of chemical reactions that process information signals modulated by chemical characteristics, such as molecule concentration, type of molecules, and energy state, to propagate them from a source (transmitter node - Tx) to a destination (receiver node - Rx). Due to the bio-devices computational limitations, the synchronization scheme is mediated by a centralized infrastructure in which the main node works as a control point. Thus, in this work, a communication system comprises multiple pairs of transmitter and receiver nodes, a communication channel, and the main node (P).

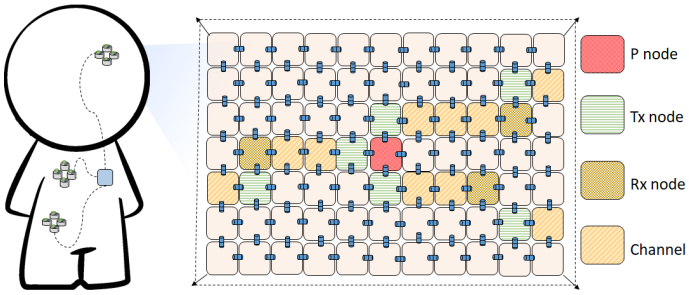

Fig. 1: Network entities distributed in a cellular tissue

Tx node is a signaling cell-based device able to encode information by the concentration of two types of information molecules (calcium ions - Ca^{2+} and inositol triphosphate - IP_3). Tx node synchronizes its internal time with a reference node (main node) after executing the synchronization procedures explained in the next subsections.

Rx node lies in a bio-device based on a signaling cell that receives the molecules and decodes the data transported by them. Rx node measures the internal concentration of molecules. In the cell, there is a set of receptors responsible for the distribution and concentration of the received molecules. Decoding is based on the concentration value with a predefined threshold detector. The multi-user interference results from the emission of molecules by other transmitters and generates inter-symbol interference when part of the transmitted signal exceeds the range initially allocated due to constant fluctuations in molecular concentrations.

Nodes follow Molecular Shift-Keying (MSK) modulation to transmit $M1$ molecules (Ca^{2+}) in bit 1 periods and transmit $M2$ molecules (IP_3) in bit 0 periods. In order to get near-error-free transmission, the network employs the binary erasure channel. As in the binary channel, Tx sends a bit with just one of two symbols (*i.e.*, 0 or 1). When Rx receives a symbol, it is known that this was, in fact, the sent symbol.

The **main node of reference** comprises a bio-device that has additional resources from the other bio-devices in the network, such as a timer to send periodically control messages, a component capable of performing cellular microstimulation that generates the open of intercellular channels (electroporation) [12] and microfluidic channels with dynamics purely driven by diffusion-reactions that control the release of molecules by concentration and type. These channels can be implemented using the microfiltration techniques [13], [14]. Each Tx node in the network detects beacons from node P. Node P broadcasts beacons (molecules concentrations) such as the synchronization request and clear-to-send messages after the synchronization phase.

Channel lies in an astrocyte cellular tissue with an area composed of i x j x k cells (c) following a three-dimensional grid organization where $c_{i,j,k}$ (i = 1, ... I; j = 1, ... J and k =

1, ... *K*) indicates the position of an arbitrary cell that contains intracellular/intercellular reactions and *N* distinguishable types of molecules $\{M_1,..., M_N\}$. The network uses IP_3 and Ca^{2+} signaling in astrocytes once these cells support the Ca^{2+} intercellular propagation up to 100μm, while propagating in a regenerative fashion [15] and reaches $450\mu m^2$ comprising about 400 cells when the calcium signaling is mechanically induced [16]. Astrocytes comprise juxtacrine signaling (that is, cell-cell contact-dependent), in which signals are transmitted along cell membranes and affect either the emitting cell or cells immediately adjacent. The Ca^{2+} and IP_3 mesoscopic-type diffusions are mediated by gap junctions that connected each cell with a maximum of six neighboring cells. The connections between the cells considered in this work are based on the study of astrocytes topologies [3].

The communication model applies the Exact Stochastic Chemical Reaction-Diffusion (ODE) solution from the Gillespie algorithm. The ODE-based simulations produce accurate variability of the chemical reactions, and it applies to study noise effects caused by inherent stochastic behavior of the chemical reactions [2]. The mathematical model of cell signaling, followed in this work, is based on experimental observations by [17]. The five fundamental blocks involved in the intracellular Ca^{2+} and IP_3 signaling process are stimulation, amplification, storage, release, and diffusion.

The stimulation stage begins with the entry of stimulating components in the cell to amplify molecules. After stimulation, IP_3 is produced by the PLC protein (Phosphoinositide phospholipase C), which leads to the increase of the Ca^{2+} concentration in the cell. Then Ca^{2+} is released from the sarco-endoplasmic reticulum into the endoplasmic reticulum and finally to the cell cytosol. Diffusion of Ca^{2+} and IP_3 ions through the cellular tissue then occurs when the gap junctions are open. Storage areas (pools) include the Ca^{2+} concentration in the cytosol, the Ca^{2+} concentration in the endoplasmic reticulum, and IP_3 concentration in the cytosol. Diffusion includes the propagation of IP_3 and Ca^{2+} molecules from one cell to another through the gap junctions. The stochastic solver computes the values of pools over time, selecting and executing scheduled reactions described.

Two cylindrical particles (connexon) form a single gap junction, one in each connecting cell. Gap junctions have biophysical properties, such as gate and conductance control, which allow or restrains the diffusion of molecules. A stochastic model for gap junction behavior was introduced in [18] and is followed in this work. The model represents voltage-sensitive gap junctions with two states of conductance for each gate: open, meaning high conductance, and closed low conductance. Thus, the possible combinations considering the states of each connexon are as follows: (i) the first connexon is in a high conductance, and the second (*i.e.*, in the adjacent cell) is in a low conductance state; (ii) both connexon in the cells are in a high conductance state; (iii) the first connexon is in a low conductance, and the second is in a high conductance. The mathematical equations that describe the cell signaling processes mentioned above were presented in [11].

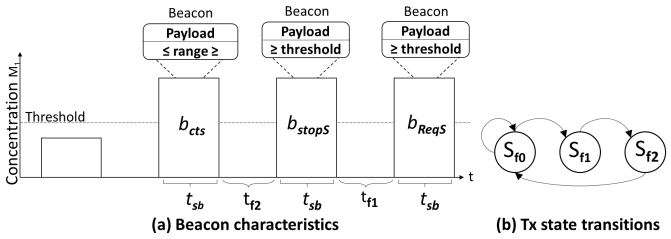

Fig. 2: Characteristics of beacons and transition state for Tx

In cell signaling, communication is unidirectional, which restricts synchronization techniques based on two-way messages: the exchange of bidirectional messages between nodes [7]. Therefore, the network nodes cannot inform the other nodes of their transmission times, intention to send a message, or when a collision occurs. Another feature is the fact that the Tx nodes cannot listen to a network common channel, only its adjacent cells (*i.e.*, in astrocytes up to six cells connected directly to the Tx by gap junctions), thus listening-based synchronization techniques (*e.g.*, one sender listens when another is transmitting and increases/decreases its internal clock) are not workable for cell signaling systems.

A. Synchronization protocol

This section details the proposed synchronization protocol considering the restrictions imposed by the molecular environment and the bio-devices computational limitations. At the current stage of the MC networks development, it can not be assumed that each node has access to Coordinated Universal Time (UTC). Therefore, conventional clock synchronization techniques are not applied. The protocol for bio-devices synchronization is initiated by the main node and follows two well-defined phases: (i) the synchronization request; and (ii) oscillations internal time setting, as described next.

Node P is not elected or selected. It is the main node by the fact that it owns other features such as a device allowing to access some global time reference, to send beacons messages periodically, an electroporation device to perform cellular stimulation that generates the open of selected intercellular channels, and microfiltration channels to direct the release of molecules. In Phase 1, node P transmits beacons releasing a predefined concentration of calcium molecules for that phase. It is unnecessary to encode any time information in the molecules. The transmitter nodes identify the beacons by the observed concentration (Fig.2a).

Beacons follow static values of time slot length t_{s_b}(*i.e.*, time period during which node P emits a specific concentration of molecules. Each Tx has an internal timer (t_i) and a time slot reserved for data transmission t_s. At the initial state, the oscillator internal timers are not synchronized (*i.e.*, state S_{f_0}) because they can start the synchronization procedure at distinct moments. Upon receiving the synchronization request beacon (b_{reqS}) from node P, the Tx nodes change their own state from S_{f0} to Sf_1 (Fig.2b). In this state, each Tx activates its t_i and records the time until the receipt of the next beacon (b_{stopS}) that signals the end of Phase 1.

At Phase 2, the Tx nodes assume the state Sf_2 indicating that their internal timer t_i are synchronized (Fig. 2b). Fig. 3 exemplifies the process of the synchronization protocol considering a cellular tissue. Transmitters are in a cell adjacent to a receiver of the previous system (*i.e.*, pairs of transmitters and receivers connected by gap junctions at a distance of approximately eight cells that play the role of channel).

Fig. 3 represents node P and the way the network grows from this node considering only one of the six directions in the 3D tissue (Tx_1, $Tx_{1\cdot2}$,...$Tx_{1\cdot n}$). Tx_1 is the only node connected to node P. Tx_1 is the reference Tx node of $Tx_{1\cdot2}$ that in turn is the reference node of $Tx_{1\cdot3}$ and so on. At the beginning of synchronization, node P sends Phase 1 broadcast beacons, passing through each cell of the channel. There is no need to encode data information into the molecules. The Tx detects beacons by their molecular concentration values. The predefined concentration thresholds for Phase 1 beacons are similar and have higher amplitude values so that beacon reached all Tx nodes in the network.

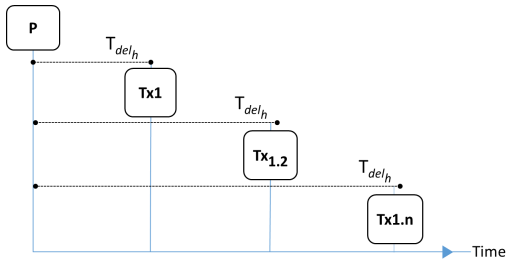

Fig. 3: Synchronization between cell signaling-based devices

Thus, when the concentration of the M_1 (calcium) molecules is greater than or equal to the predefined threshold (*i.e.*, B_{F1} if $M_1 \geq$ threshold) the Tx node identifies that it is a Phase 1 beacon and changes its own state according to the previous state (*i.e.*, (*i*) State Sf_0, (*ii*) State Sf_1, and (*iii*) State Sf_2). Beacons b_{reqS} and b_{stopS} have the same time slot length (t_{s_b}) reserved for the symbol transmission and they respect a time interval (t_{f1}) defined according to the time required for the synthesis of molecules at Tx nodes. As the distance between node P and a node Tx increases, the longer is the propagation delay time between beacons b_{reqS} and b_{stopS}.

Considering the example presented in Fig. 3, the instant of time for the concentration threshold to be identified in node $Tx_{1\cdot2}$ is considered to be the instant of receipt of the beacon message. The propagation delay is denoted by t_{del_h}, where $h \epsilon \{P,\ Tx_{1\cdot2}\}$. In Phase 2, node Tx_{12} infers its internal timer according to the equation $k = t_s + t_{del_{Tx_{1.2}}}$, which indicates how many units of time node $Tx_{1\cdot2}$ must wait before starting the data transmission. Since the k value of the $Tx_{1\cdot2}$ node is greater than the value of k on its reference transmitter node, it only starts transmitting when the Tx_1 node finishes data communication with its respective receiver.

After the synchronization step, node P sends CTS (clear-to-send) messages as a medium access control. There is no need to encode data in CTS messages, the transmitters nodes that are synchronized identify these messages by the observed molecular concentration. Thus, when the concentration of the M_1 (*i.e.*, calcium) molecule is contained in the predefined range (b_{cts} if conc $\epsilon\ R/\{tx_{m1} \geq x \leq tx_{m1}\}$), each Tx node in the Sf_2 state recognizes this message as the b_{cts} beacon.

CTS messages are directed on the channel using the electroporation feature to stimulate only the gap junctions in a given direction and microfiltration channels to send the control molecules only to the selected channels. This feature prevents transmitter nodes close to or connected to node P from producing multi-user interference with each other. So there is no need to wait for all bio-devices from one direction to transmit before releasing the opposite direction. Upon receiving the CTS message, all Tx nodes in a given direction activate their internal timers and start the countdown to initiate the coding and data transmission.

Given the computing limitations of bio-devices, simple error control schemes are necessary for cell signaling-based channels. The binary modulation technique uses concentrations of two not dependent types of information molecules to discriminate the bit-0 from the bit-1 in a binary erasure channel to reduce the ISI. The network operates with positive concentration values for each molecule based on a predefined range, and any value belonging to the range being means the bit 1 (Ca^{2+}) or the bit 0 (IP_3), according to the molecule whose concentration was measured. Different molecules represent each bit to reduce the probability of ISI or noisy molecules coming from neighboring cells (*i.e.*, generated by the stochastic behavior of the chemical reactions or that get in the cell due to stochastic behavior of the gap junction). Transmitter decides which molecule to send depending on the data message. Time steps are discretized into time-slots (of duration t_b) for a single symbol transmission, based on the propagation time. The emission occurs at the beginning of a symbol time interval. The decoding process is based on the molecular concentration value with a predefined threshold detector and occurs at the receiver side (Eq. 1).

$$RXdecode(s) = \begin{cases} 1 & \text{if } M_1(s)\ X\ \epsilon\ R/\{r_{m1} \geq x \leq r_{m1}\} \\ 0 & \text{if } M_2(s)\ X\ \epsilon\ R/\{r_{m2} \geq x \leq r_{m2}\} \end{cases} \quad (1)$$

Receiver identifies whether the concentration has reached the predefined concentration range per type of molecule in each symbol duration to determine the sent symbol.

IV. Evaluation

This section describes the performance evaluation of the proposed synchronization protocol. The next subsections detail the simulation environment and discuss the results.

A. Description of the simulation environment

The simulations follow a stochastic model based on the Gillespie [10] algorithm to determine the concentration of molecules of each pool of Ca^{2+} and IP_3 over time [11]. At each time step, the algorithm selects a random cell; a random internal reaction of that cell also schedules a time step for each one of them. The choice of reaction follows the roulette wheel selection process, which selects the events based on

their probability values. The effect of executing a reaction is a change in the values of the pools *i.e.*, according to the reaction-diffusion ODEs. A constant changes the value of the set according to the positive or negative result of the reaction.

The convergence time (*i.e.*, time a network takes for all nodes to get synchronized) evaluates the synchronization protocol performance. The analysis assumes a network size from 12 to 60 active signaling cells, herein called nodes, with an increment of 12 per scenario. The passive signaling cells play a role in the communication, as they are relay nodes that push the molecules to their neighbor cells using an input of signals from nodes. The transmitter-receiver distance is eight cells. To evaluate the molecules concentration thresholds for the synchronization protocol and data coding, as well as the time slots (of duration T_b) for single symbol transmission, the following metrics were investigated: (i) the oscillation of the spatio-temporal concentration of Ca^{2+} and IP_3 molecules in Tx and Rx, (ii) the signal-to-noise ratio based on the study [19], (iii) the end-to-end capacity (based on Shannon's entropy) versus T_b analysis with respect to varying distances and (iv) the propagation delay.

B. Results

In order to determine concentration threshold values for the encoding mechanism and the synchronization protocol, the molecular spatio-temporal concentration for each molecule was investigated. Figs. 4a and 4b show the simulation results for Tx, Rx and destination noise concentrations values versus time in a 3D astrocyte tissue. The natural oscillation frequency of the concentration levels in astrocytes is 0.1Hz. The Rx concentration is 500 nM, the Tx initial concentration is 2×10^3 nM and the distance is 8 cells. The amplitude of oscillations is 2.5 μm for IP_3 and 0.6 μm for Ca^{2+}. Based on the concentration levels alone, one observes different behaviors. A meaningful observation lies in the different maximum concentration rates for each molecule. However, Rx concentration levels may be higher due to noise caused by constant and random fluctuations in the concentrations of IP_3 and Ca^{2+}. The intracellular noise of the Ca^{2+} molecule reaches a concentration of 0.13 nM, while the IP_3 noise reaches a maximum concentration of 0.18 nM. It is important to note that these results consider only the molecule noise concentration.

Fig. 4d presents the results for the propagation delay and the end-to-end capacity versus t_b analysis concerning varying distances in the number of cells. The initial calcium concentration at Tx is 2000 nM and at 100000 nM at Rx. The oscillation frequency is 1kHz. The amount of Ca^{2+} transmitted is measured compared to the Ca^{2+} received over time to reasonably estimate the delay for each sends symbol. The propagation delay is more significant when the distance is greater than three (20.3%), explained by Ca^{2+} regeneration in the astrocyte that produces and releases new molecules, delaying the initial pulse. The delay analysis does not consider a time interval (T_b) to transmit the pulse. The analysis of capacity versus T_b shows that increasing the T_b slightly increases the information capacity (15%). This occurs because the inter-symbol interference effects reducing, allowing conveying of more information for a longer time.

Considering the propagation delay and end-to-end capacity results got, the following time intervals were set, for data encoding the T_b is 300s and for the synchronization protocol t_{s_b} is 50s with intervals of t_{f_1}=10s and t_{f2}=40s. For encoding data, the time slots are longer to avoid inter-symbol interference and shorter for the synchronization protocol because it is unnecessary to encode data in the beacon and reduce delay propagation. The concentration thresholds for the decoding process in the Rx nodes were defined for Ca^{2+} *i.e.*, Bit-1 if M_1 X ϵ R/{0.15nM – 0.25nM} and IP_3 *i.e.*, Bit-0 if M_2 X ϵ R/{0.18nM – 1nM} based on the spatio-temporal concentration results. Tx nodes identify the synchronization beacons by the concentration threshold B_{F1} if $M_1 \geq$ 0.3nM, and synchronized Tx nodes identifies clear-to-send beacons by the interval B_{cts} if conc ϵ R/{0.4nM – 0.6nM}.

Fig. 5a presents the results for the average convergence time in relation to different network sizes. The larger the size of the network (*i.e.*, number of Tx nodes), the slower is the synchronization process (*i.e.*, approximately 1000s for a network size of 60 nodes which comprises 30 Tx nodes). However, this is not necessarily associated with the number of nodes synchronized but with the time needed for the beacon pulse resonance, which depends on the characteristics of the MC channel. Although the time values for convergence are higher compared to conventional systems, they are congruent for cell signaling systems.

Fig. 5b presents the results for the convergence time concerning the number of hops. This analysis considers the Tx nodes of only one of the six directions in the 3D tissue. The number of hops refers to the number of cells that the signal needs to travel. Results show that the distance between node P and node Tx plays an important role in the synchronization; the greater is the distance, the slower the convergence is. The network with six Tx nodes (*i.e.*, twelve-node network size) has the shortest time to converge; this is because, in the first hop, the Tx nodes directly connected to node P. The exchange of synchronization messages is carried out essentially by broadcast from node P to Tx nodes. It does not require the exchange of two-way messages, reducing the number of beacons supporting the protocol operation, i.e., two synchronizations beacons and six CTS beacons.

Fig. 5c presents the results for the bit error probability versus the molecular signal-to-noise ratio (E_b/N_0). This analysis considers two modulation techniques, the MSK modulation technique with distinct molecules to discretize the symbols, i.e., calcium for bit 1 and IP_3 for bit 0 with and the OOK modulation that uses only the IP_3 to transmit molecules in periods of bit 1 and not transmit molecules for bit 0 (the concentration is zero). The results were collected after the transmission of the 1.0.1 bits. Using different molecules to discretize the symbols has better performance as E_b/N_0 increases in the channel and benefits the communication system, decreasing the probability of bit error. The results of the signal-to-noise ratio (Fig. 4c) support the use of different types of molecules to

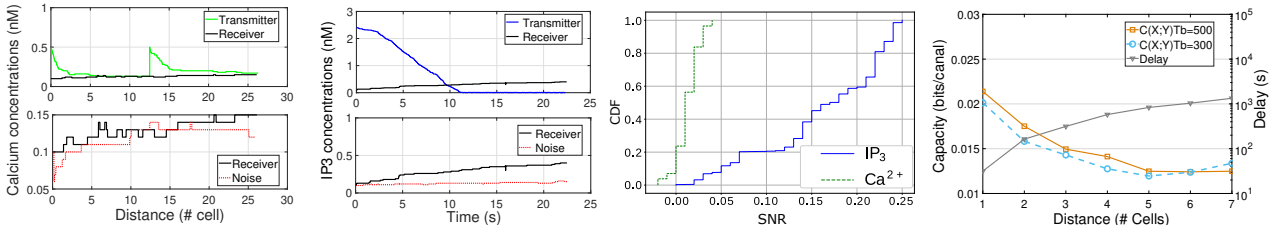

(a) Ca^{2+} concentrations (b) IP_3 concentration (c) Signal-to-noise ratio (d) Capacity and Delay

Fig. 4: Ca^{2+} and IP_3 molecular concentrations, signal-to-noise ratio, propagation delay and end-to-end capacity

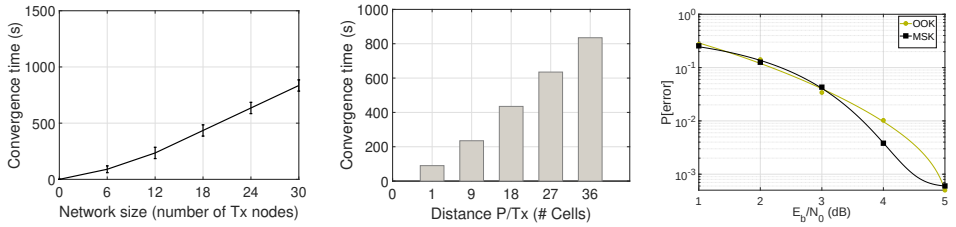

(a) Convergence time: Tx number (b) Convergence time: hops (c) Error probability

Fig. 5: Analyzing the synchronization protocol over network size variation and the bit error probability

differentiate the symbols since the values of overlap between the concentrations of molecules are low (less than 10%), which reduces the likelihood of interference between symbols during the encoding process.

V. Conclusion

This paper presented a synchronization protocol for multi-user molecular communication between signaling cells. The synchronization process is mediated by a centralized infrastructure in which one bio-device serves as the control point for the entire network. This is motivated by computational limitations in bio-devices and by the fact that cell-to-cell communication is essentially unidirectional. The protocol signaling occurs by pulse resonance. This information allows transmitter bio-device to adjust their internal timers and achieve convergence. Centralized synchronization can pave the way to networks constructed from molecular communication links. As future works, it is expected to explore scenarios considering multiple main nodes and medium access control.

References

[1] I. F. Akyildiz, M. Pierobon, S. Balasubramaniam, and Y. Koucheryavy, "The internet of bio-nano things," *IEEE Commun. Magazine*, vol. 53, no. 3, pp. 32–40, 2015.

[2] T. Nakano and J.-Q. Liu, "Design and analysis of molecular relay channels: An information theoretic approach," *IEEE Trans. on NanoBioscience*, vol. 9, no. 3, pp. 213–221, 2010.

[3] J. Lallouette, M. De Pittà, E. Ben-Jacob, and H. Berry, "Sparse short-distance connections enhance calcium wave propagation in a 3d model of astrocyte networks," *Frontiers in Comp. Neurosci.*, vol. 8, p. 45, 2014.

[4] A. C. Heren, M. S. Kuran, H. B. Yilmaz, and T. Tugcu, "Channel capacity of calcium signalling based on inter-cellular calcium waves in astrocytes," in *The 3rd IEEE International Workshop on Molecular and Nano Scale Communication*, 2013.

[5] M. T. Barros, P. Doan, M. Kandhavelu, B. Jennings, and S. Balasubramaniam, "Engineering calcium signaling of astrocytes for neural–molecular computing logic gates," *Scientific reports*, vol. 11, no. 1, pp. 1–10, 2021.

[6] E. Shitiri, H. B. Yilmaz, and H.-S. Cho, "A time-slotted molecular communication (ts-moc): Framework and time-slot errors," *IEEE Access*, vol. 7, pp. 78 146–78 158, 2019.

[7] L. Lin, W. Li, R. Zheng, F. Liu, and H. Yan, "Diffusion-based reference broadcast synchronization for molecular communication in nanonetworks," *IEEE Access*, vol. 7, pp. 95 527–95 535, 2019.

[8] V. Jamali, A. Ahmadzadeh, and R. Schober, "Symbol synchronization for diffusive molecular communication systems," in *IEEE International Conference on Communications (ICC)*. IEEE, 2017, pp. 1–7.

[9] M. J. Moore and T. Nakano, "Oscillation and synchronization of molecular machines by the diffusion of inhibitory molecules," *IEEE Trans. on Nanotec.*, vol. 12, no. 4, pp. 601–608, 2013.

[10] D. T. Gillespie, "Exact stochastic simulation of coupled chemical reactions," *The J. of physical chemistry*, vol. 81.

[11] L. F. Borges, M. T. Barros, and M. Nogueira, "A multi-carrier molecular communication model for astrocyte tissues," in *IEEE International Conference on Communications (ICC)*. IEEE, 2020, pp. 1–6.

[12] S. K. Frandsen, M. Vissing, and J. Gehl, "A comprehensive review of calcium electroporation—a novel cancer treatment modality," *Cancers*, vol. 12, no. 2, p. 290, 2020.

[13] L. J. Zeman and A. L. Zydney, *Microfiltration and ultrafiltration: principles and applications*. CRC press, 2017.

[14] B. C. Akdeniz and M. Egan, "Molecular communication for equilibrium state estimation in biochemical processes on a lab-on-a-chip," *IEEE Trans. on NanoBiosc.*, 2021.

[15] N. Kuga, T. Sasaki, Y. Takahara, N. Matsuki, and Y. Ikegaya, "Large-scale calcium waves traveling through astrocytic networks in vivo," *Journal of Neuroscience*, vol. 31, no. 7, pp. 2607–2614, 2011.

[16] J. L. Peters, B. J. Earnest, R. B. Tjalkens, V. M. Cassone, and M. J. Zoran, "Modulation of intercellular calcium signaling by melatonin in avian and mammalian astrocytes is brain region-specific," *Journal of Comparative Neurology*, vol. 493, no. 3, pp. 370–380, 2005.

[17] M. Lavrentovich and S. Hemkin, "A mathematical model of spontaneous calcium (ii) oscillations in astrocytes," *Journal of Theoretical Biology*, vol. 251, no. 4, pp. 553–560, 2008.

[18] S. Baigent, J. Stark, and A. Warner, "Modelling the effect of gap junction nonlinearities in systems of coupled cells," *Journal of theoretical biology*, vol. 186, no. 2, pp. 223–239, 1997.

[19] G. Yu, M. Yi, Y. Jia, and J. Tang, "A constructive role of internal noise on coherence resonance induced by external noise in a calcium oscillation system," *Chaos, Solitons & Fractals*, vol. 41, no. 1, pp. 273–283, 2009.